Nanoscale

PAPER

View Article Online
View Journal | View Issue

Cite this: *Nanoscale*, 2017, **9**, 4810

Morphological and chemical transformations of single silica-coated CdSe/CdS nanorods upon fs-laser excitation†

Wiebke Albrecht,* [a] Bart Goris,[b] Sara Bals,[b] Eline M. Hutter,[a] Daniel Vanmaekelbergh,[a] Marijn A. van Huis[a] and Alfons van Blaaderen*[a]

Received 23rd December 2016,
Accepted 17th March 2017

DOI: 10.1039/c6nr09879g

rsc.li/nanoscale

Radiation-induced modifications of nanostructures are of fundamental interest and constitute a viable out-of-equilibrium approach to the development of novel nanomaterials. Herein, we investigated the structural transformation of silica-coated CdSe/CdS nanorods (NRs) under femtosecond (fs) illumination. By comparing the same nanorods before and after illumination with different fluences we found that the silica-shell did not only enhance the stability of the NRs but that the confinement of the NRs also led to novel morphological and chemical transformations. Whereas uncoated CdSe/CdS nanorods were found to sublimate under such excitations the silica-coated nanorods broke into fragments which deformed towards a more spherical shape. Furthermore, CdS decomposed which led to the formation of metallic Cd, confirmed by high-resolution electron microscopy and energy dispersive X-ray spectrometry (EDX), whereby an epitaxial interface with the remaining CdS lattice was formed. Under electron beam exposure similar transformations were found to take place which we followed *in situ*.

Introduction

Heterostructured semiconductor nanoparticles (NPs) have attracted much scientific attention due to their tunable optical and electronic properties.[1,2] They display unique size and material dependent emission and absorption properties that are of great interest for various applications such as light-emitting diodes (LEDs),[3] lasers,[4–6] sensors[7] and biological imaging.[8] Among the vast array of morphologies of heterostructured semiconductor NPs, CdSe/CdS nanorods (NRs) are intriguing systems as they exhibit quantum yields up to 75% and reduced blinking.[9–11] Such NRs consist of a spherical CdSe core and an elongated CdS shell in which the core is asymmetrically positioned towards one end of the rod. The charge separation of the carriers can be influenced by depositing a metallic centre which is used for electro-optical modulators,[12] optical switches,[13] nano-thermometers,[14] photocatalysis[15,16] and photovoltaics.[17] The emission and absorption are polarized which can be exploited in polarized LED's[18] but could also be used in improved data storage as has been demonstrated for gold nanorods.[19] Furthermore, the extinction coefficients for multiple photon absorption in CdSe/CdS NRs are significantly higher than for CdSe quantum dots making them interesting for non-linear optical applications as well.[20,21]

For many applications, the chemical and (photo)thermal stability of CdSe/CdS NRs is still a serious issue. Several solutions were proposed to overcome the stability problems. In particular, complex multishell heterostructures, such as CdSe/CdS/ZnS, proved promising but require a more complicated synthetic procedure.[8,22,23] Alternatively, a silica coating is known to enhance the thermal and colloidal stability of NPs and dyes.[24–27] This has also recently been shown for CdSe/CdS NRs where a silica coating resulted in increased photostability under UV irradiation and chemical stability under O_2 exposure with respect to the same uncoated NRs.[28] It has not been explored so far, however, how chemically and morphologically stable silica-coated CdSe/CdS NRs are upon irradiation, when *e.g.* exposed to an electron beam or to fs-laser pulses which are used in several applications and/or particle characterization methodologies. This is important to study since different morphological modifications of the particles under study can result in completely new structures. It was shown, for example, that Au-tipped CdS NRs underwent chemical transformations

[a]*Debye Institute for Nanomaterials Science, Utrecht University, Princetonplein 5, 3584 CC Utrecht, The Netherlands. E-mail: W.Albrecht@uu.nl, A.vanBlaaderen@uu.nl*

[b]*Electron Microscopy for Materials Science (EMAT), University of Antwerp, Groenenborgerlaan 171, 2020 Antwerp, Belgium*

†Electronic supplementary information (ESI) available: Experimental methods, (S)TEM images of silica-coated NRs before and after fs-laser excitation, impact on uncoated and not fully covered NRs, lattice spacings of CdS and Cd, electron beam influence on fragments, additional EDX maps. See DOI: 10.1039/C6NR09879G

upon high-density electron beam irradiation exhibiting new phases that would not be stable in bulk.[29] Such transformations were not observed for NRs without a Au-tip or when the NRs were simply heated without radiation-induced effects.[29,30] Such radiation-induced modifications are interesting from a fundamental point of view but also for stability reasons. Understanding the interaction of these systems in silica shells also helps to design and optimize silica-coated hybrid metal–semiconductor structures.[31] Additionally, contrary to sphere-like quantum dots, NRs often have a non-equilibrium shape which plays an important role regarding stability as is seen for gold NRs for which the metastable shape is unstable at temperatures far below the melting temperature.[32] Studying such changes and transformations can reveal novel nanostructures and interesting nanoscale phenomena.

We performed fs two-photon excitation experiments on silica-coated CdSe/CdS NRs and monitored the structural changes of individual particles after fs-pulse excitation. The experiments were conducted at different laser intensities while analyzing the same particles before and after fs-laser excitation with transmission electron microscopy (TEM). We observed that with increasing laser power the particles first broke into two or more anisotropic fragments which then independently deformed into a more spherical shape. Additionally, Cd-rich domains were formed out of the remaining (mainly) CdS phase which was revealed by high-resolution scanning transmission electron microscopy (STEM) and EDX. While very similar results were obtained under electron beam excitation, heating did not result in such transformations. These findings are different in comparison to the same NRs without a silica-coating or with only a partial coating, where we found sublimation of CdS without deformation, showing that physical confinement can dictate morphological and chemical changes.

Experimental methods

The CdS NRs with a spherical CdSe core were synthesized following a seeded growth approach.[9] The rods were 46 nm ± 4 nm long and 4.6 nm ± 0.6 nm thick and had a CdSe core size of 3.2 nm. A silica shell of about 10 nm was grown around the CdSe/CdS NRs following Hutter *et al.*[33] The absorption and emission as well as TEM images of these NRs before and after silica growth are presented in Fig. 1. The first absorption peak of the CdS shell was at 460 nm. Due to the larger volume of the shell compared to the core, absorption is governed by the CdS shell[34] whereas emission stems from the CdSe core and is red-shifted as CdSe has a smaller band gap than CdS. For the femtosecond laser excitation a Leica SP8 confocal setup with an integrated Ti:Sapphire laser (Coherent chameleon II, 80 MHz repetition rate, 140 fs pulses) was used where the particles could be found back on the TEM grids. The Ti:Sapphire laser can be tuned from 670 nm to 1080 nm. We chose 920 nm as excitation wavelength since it mimicks a two-photon excitation of the NRs. A thin 3D stack was scanned with a pixel size of 22.6 nm × 22.6 nm pixel size, a pixel dwell time of 1.2 μs and a total scan time of about 20 s. Details can be found in the ESI.†

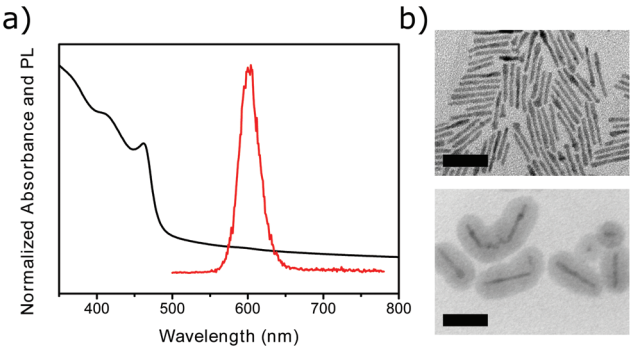

Fig. 1 Absorption, luminescence (a) and TEM images of uncoated and silica-coated CdSe/CdS nanorods (b). The scale bar corresponds to 50 nm.

Results and discussion

In order to study the structural changes of the CdSe/CdS NRs after fs-laser excitation, different laser fluences were applied and morphological changes were observed by TEM. The upper row in Fig. 2a shows the particles before laser excitation and the second row displays the same particles after fs-laser excitation of different fluences. For the lowest applied peak fluence of 2.6 mJ cm^{-2} the particles did not change their shape as displayed in the first column of Fig. 2a. At the highest fluence of 8.7 mJ cm^{-2} most semiconductor NRs sublimated leaving empty silica shells behind as can be seen in the last column in Fig. 2a. Interestingly, after fs-excitation with an in-between laser fluence of 5.8 mJ cm^{-2} differently shaped semiconductor particles were found in a mostly intact silica shell as shown in the two middle columns in Fig. 2a. In some cases (arrows in left column) the NRs broke into 2 rods with about half of the length of the original rod keeping a thickness of about 5 nm. In other cases two shorter fragments of increased thickness (about 6.5 nm) were found inside the silica shells, as highlighted by the upper arrow in the right column. These fragments deformed as their shape was more spheroidal than rod-like. Spherical fragments with diameters of about 8 nm were also found as shown in the right column of the middle box in Fig. 2a (lower arrow). The NRs mainly fragmented into two pieces although one or three and sometimes more than 3 fragments were also observed (Fig. S2†). The deformed particles most likely decreased in volume as estimated from comparing the volume of the same rod before and after fs-laser excitation indicating that the CdS partially decomposed and/or sublimated to some extent as well at the intermediate fluence and not only at the highest one shown in Fig. 2a. However, this needs to be considered with care since TEM images are just 2D projections.

The silica shells have a stabilizing effect, almost certainly of kinetic origin, at least against the sublimation of CdS, since the

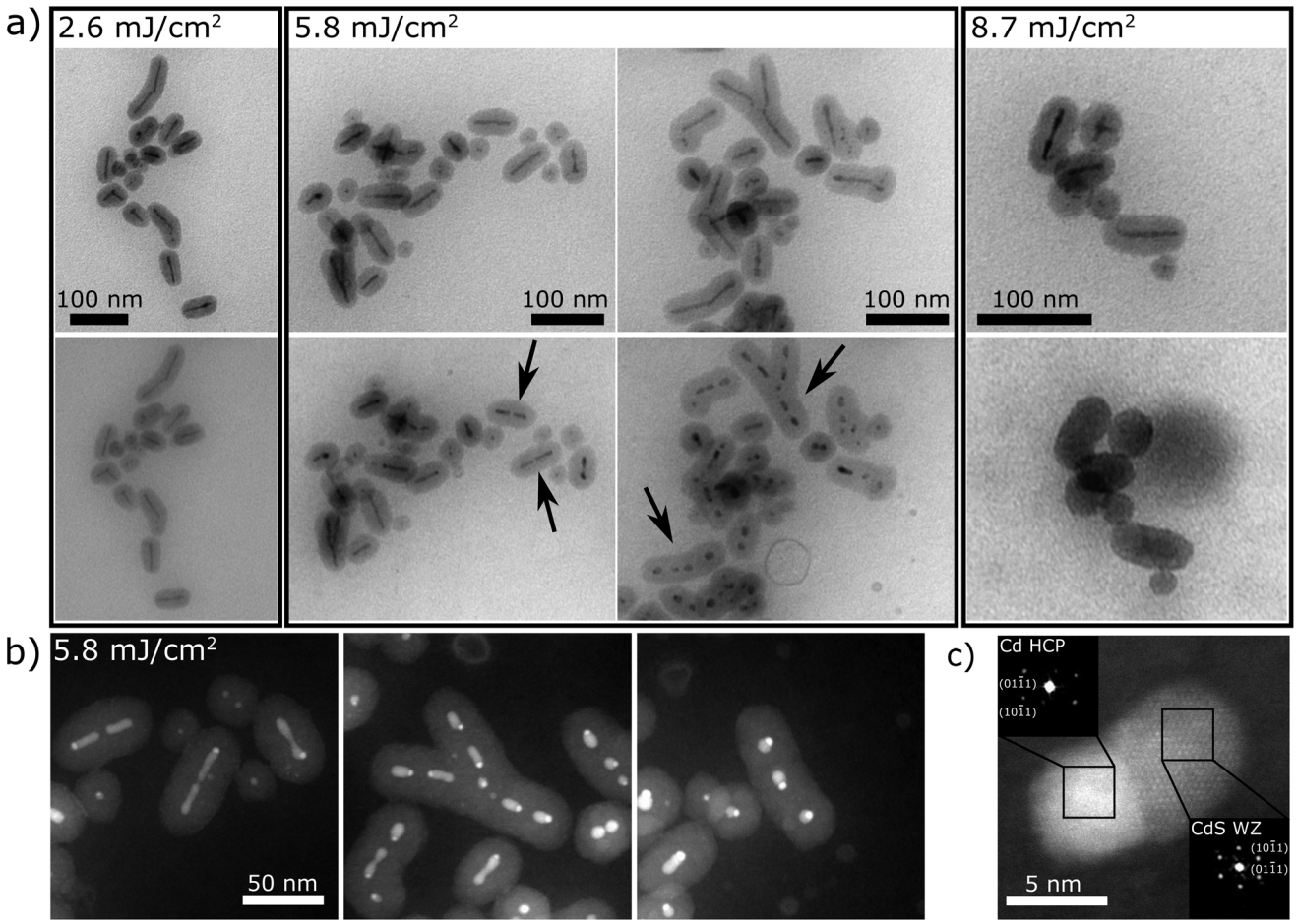

Fig. 2 Deformation stages at different laser fluences. (a) TEM images of the same silica-coated CdSe/CdS NRs before (top row) and after (bottom row) excitation with fs-laser pulses of three different peak fluences. The arrows mark examples of three different shapes found after illumination. (b) HAADF-STEM images of the three different shapes obtained after excitation with 5.8 mJ cm^{-2} pulses. (c) HR-STEM image of a typical fragment. The insets show two diffractograms corresponding to the two different parts of the fragment (see text for details).

same uncoated NRs disappeared even under the lowest fluence of 2.6 mJ cm^{-2} (Fig. S4a†). The same was true for particles where the silica did not fully cover the NR which allowed for easier sublimation (Fig. S4b†). The latter indicates that the observed breaking and deformation only happened because of the confinement of the silica shell since it delayed the evaporation of CdS forcing the system to react to the absorbed energy in a different way. Breaking up of the semiconductor NRs was not observed for uncoated NRs in our experiments and in *in situ* heating experiments of uncoated CdSe NRs.[30] The deformation of uncoated CdSe/CdS NRs to a spherical shape under fs-pulse excitation was observed previously.[35] However, from these experiments it was not clear whether these were remnants of sublimated NRs and/or really deformed fragments of the original NRs.

In order to obtain a better understanding of the morphological transformations observed in Fig. 2a, STEM and EDX measurements were performed as well. STEM images of the different particle shapes are presented in Fig. 2b. The left and middle images in 2b show a close-up of some particles from the middle columns in Fig. 2a. In most cases (but certainly not all), and especially for the semiconductor particles within the shells that were more deformed after fs-excitation, a bright spot was observed at the tips of the fragments. The spot increased relatively in size with respect to the remaining particle/fragment for higher deformation degrees as shown in Fig. 2b. Inherent to imaging in high-angle annular dark-field (HAADF) STEM mode is the *z*-contrast whereby heavier elements appear brighter. Thus, the bright spots cannot be CdS or CdSe as these would have a similar STEM contrast. Pure Cd would give a higher STEM contrast. To verify the presence of metallic Cd a high-resolution STEM image was taken of such a fragment. The image together with diffractograms of both parts of the fragment are shown in Fig. 2c. For the less bright part of the fragment (right diffractogram) we obtained lattice spacings of 0.310 nm and 0.299 nm. These are in reasonable agreement with the calculated values of 0.318 nm for the (10$\bar{1}$1) and (01$\bar{1}$1) lattice spacings in wurtzite CdS (details in ESI†). Notably, the lattice was slightly tilted since the two measured values are not the same. For the bright part of the fragment (left diffractogram) we obtained spacings of

0.225 nm and 0.218 nm which corresponds to the calculated spacings of 0.235 nm for the $(10\bar{1}1)$ and $(01\bar{1}1)$ planes for hexagonal close-packed Cd. Similar to the CdS lattice the crystal was slightly tilted. Thus, the high-resolution STEM image confirms that metallic Cd segregated at the tips of the NRs. Interestingly, both lattices were found in the same crystallographic orientation. This shows that laser annealing can lead to an epitaxial, strong and extended metal–semiconductor interface, an important topic in nanoscience.[36,37] Possibly a similar 'fs-laser-writing' methodology can be applied to create epitaxial interfaces with other hcp metals such as Mg, Ti, Co or Zn. This cannot be simply achieved by heating the NPs as we did not observe such transformation during *in situ* heating experiments indicating that the type of energy deposition matters (Fig. 4). The location of the segregated Cd spots was observed to be often located at one end of the original CdSe/CdS NR and the formed fragments. We did not observe a preference of Cd segregated spots of neighboring fragments to point toward or away from each other.

In order to further confirm whether the segregated parts were Cd we performed STEM–EDX chemical mapping measurements on these particles. Fig. 3a and b show the count rate maps for the particles also shown in the middle and right images in Fig. 2b, respectively. The EDX measurements confirmed that the brighter spots observed with STEM were indeed Cd, whereas the rest of the particle was CdS. The Se which is in principal present in the core of the particles could not be mapped (Fig. S7†). That does not necessarily mean that no Se was present anymore. Due to the beam sensitivity of the material the EDX maps could only be taken for a relatively short time (306 s and 210 s for the maps in Fig. 3a and b, respectively). Since the core is only 3 nm small this might not be enough time to acquire sufficient counts to detect the Se. It is good to mention that under similar EDX acquisition conditions the CdSe core could also not be detected for undeformed silica-coated NRs (Fig. S8†). For that reason the core position is normally determined by elaborate analysis of high-resolution TEM or STEM images.[9,38] It is known, however, that the core of core/shell semiconductor nanoparticles can oxidize and consequently shrink upon heating or irradiation.[39,40] Thus, although the impact of laser heating is different to oven or *in situ* heating, it would not be surprising if the core was not present anymore after the applied 5.8 mJ cm^{-2} laser pulses. The three marked fragments in Fig. 3a and all fragments in Fig. 3b were quantified with the Cliff–Lorimer method. Whereas the fragments in Fig. 3a

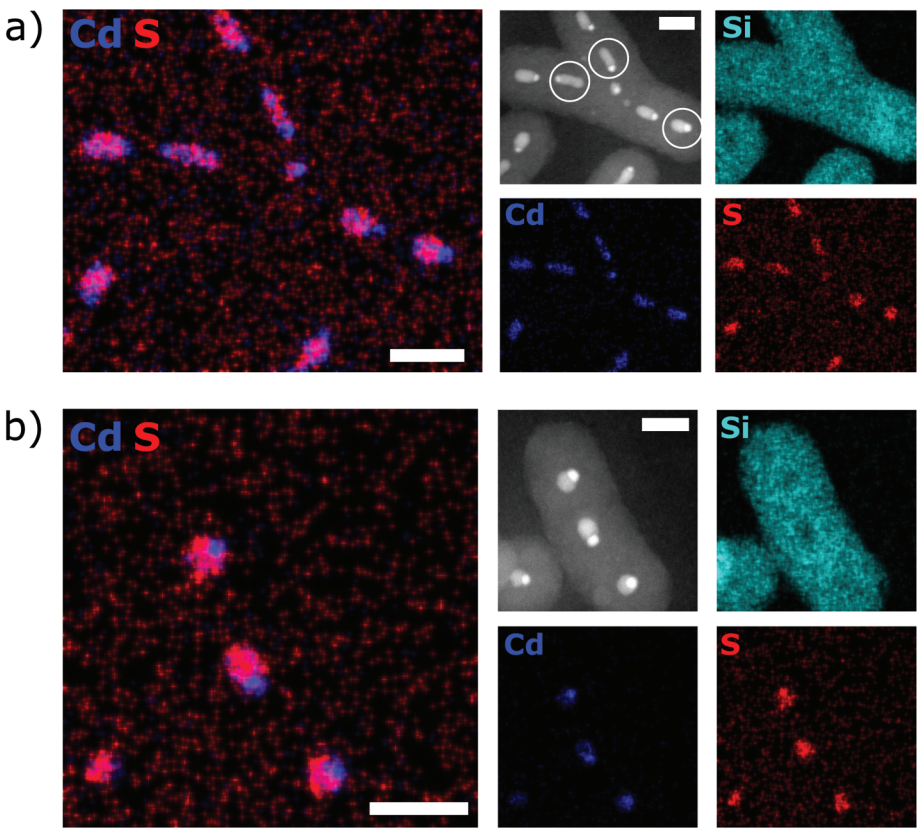

Fig. 3 Results of STEM–EDX chemical mapping performed on the fragments obtained after fs-excitation. (a) HAADF-STEM image and count rate maps of Cd, S, Si and the overlay of Cd and S for spheroidal fragments obtained after excitation with 5.8 mJ cm^{-2} as shown in the middle image in Fig. 2b. By quantification of the three circled fragments we obtained a Cd : S ratio of about 50 : 50. (b) HAADF-STEM image and count rate maps of Cd, S, Si and the overlay of Cd and S for spherical fragments obtained after excitation with 5.8 mJ cm^{-2} as shown in the right image in Fig. 2b. Quantification of the fragments revealed a Cd : S ratio of 56 : 44. All scale bars represent 20 nm.

exhibited a Cd : S ratio of 50 : 50, which is similar to the Cd : S ratio of the undeformed silica-coated NRs (see Fig. S8† for details), the fragments in Fig. 3b contained an excess of Cd with a Cd : S ratio of 56 : 44, which is expected due to an increased amount of segregated Cd.

On a side note but worth mentioning, under kHz excitation conditions uncoated CdSe/CdS NRs of similar size were shown to withstand higher fluences as shown for two-photon pumped amplified spontaneous emission experiments.[2,6] Furthermore, for data storage experiments under MHz excitation, *i.e.* where the inhibition of luminescence is desired, the amount of absorbed pulses played a role as well.[35] Thus, heat accumulation is an important factor for the photostability of CdSe/CdS NRs for high repetition rate lasers.

However, the chemical and morphological transformations observed here are not purely heat-induced as *in situ* heating experiments only lead to sublimation of the material without CdS decomposition. Fig. 4 presents results of heating experiments performed *in situ* in an electron microscope. Fig. 4a shows STEM images of the same spot followed over different temperatures. The indicated time is the heating time at that temperature when the STEM image was taken. The zoom was kept at relatively low magnification to avoid electron-beam induced deformation of the NRs as shown in Fig. 5. The particles were unchanged up to 400 °C. At 450 °C particles started to sublimate and sublimation increased with temperature. At 700 °C about half of the particles sublimated whereas the rest remained almost completely intact. The particles that sublimated were mainly NRs that were not fully covered by the silica shell, similarly to the fs-laser excitation (Fig. S4†). It is remarkable that most particles that were fully covered by the silica shell stayed stable up to such high temperatures although it is known that the thermal stability drastically decreases for nanomaterials.[41,42] However, it is known that the electron beam can cause the deposition of a thin carbon shell around the particles which stabilizes them tremendously. Such

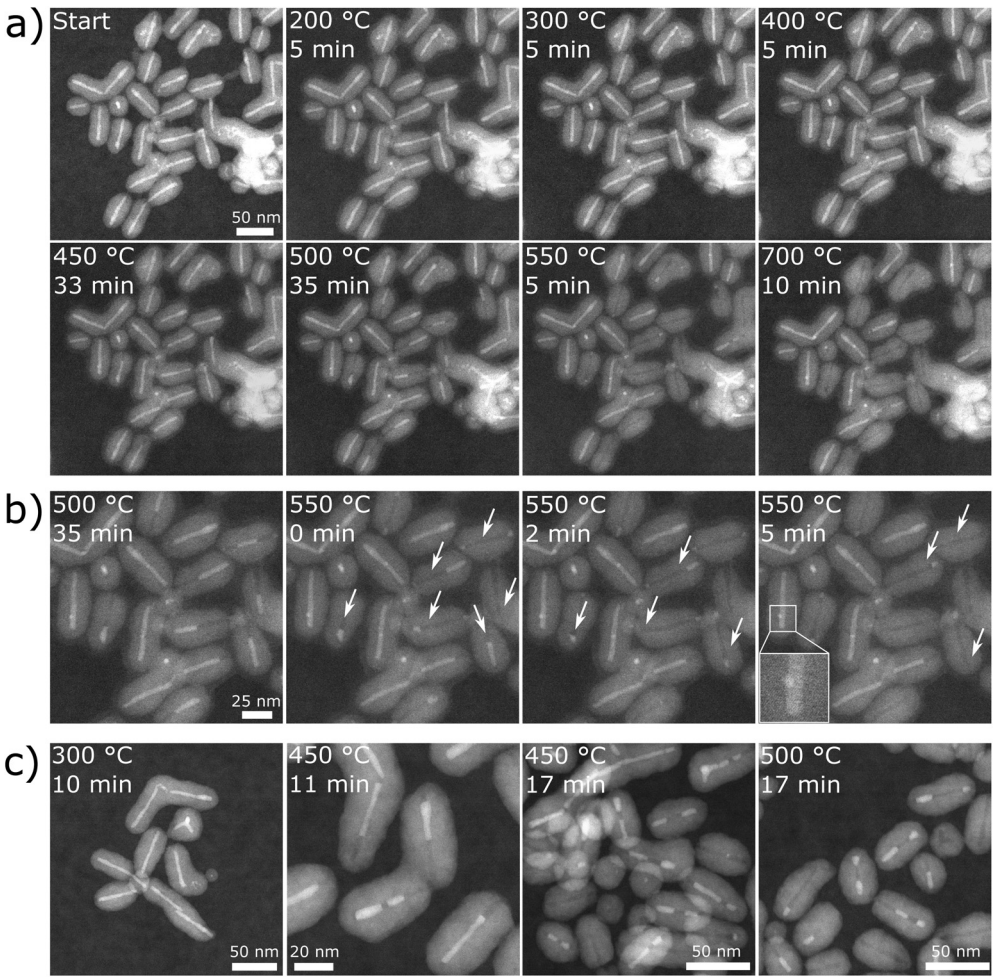

Fig. 4 *In situ* heating experiments in the electron microscope. (a) STEM images of the same spot at different heating temperatures and times. The indicated time is the heating time at that temperature. (b) Zoomed-in STEM images of the spot in (a) which were taken subsequently after either increasing the temperature or after advanced time. The electron beam was always blanked between all images that were taken. The white arrows mark NRs that exhibit advanced sublimation compared to the same NR in the prior image. (c) STEM images of different windows that were not exposed to the electron beam before heating at the indicated temperature and time.

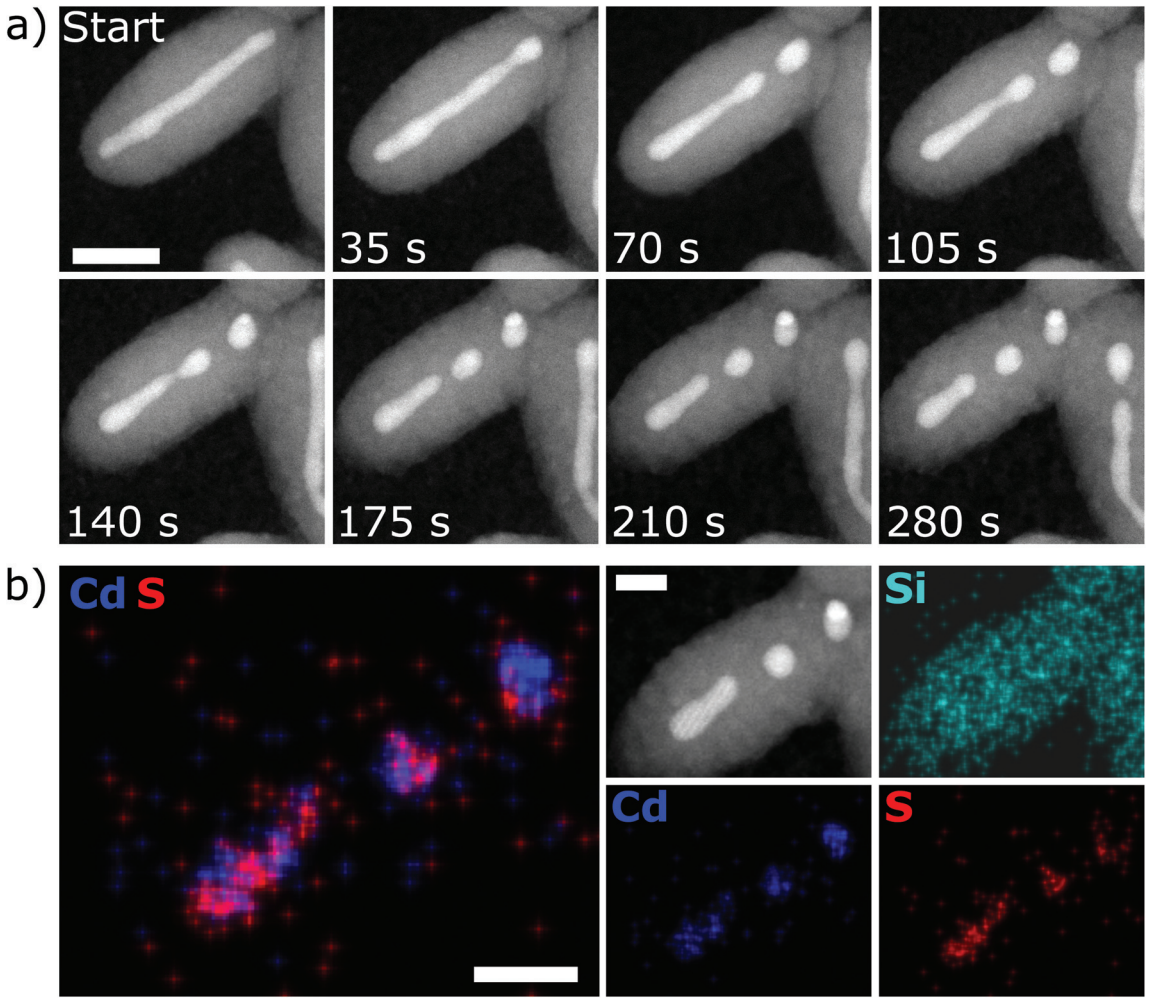

Fig. 5 *In situ* deformation of a silica-coated CdSe/CdS NR induced by the electron beam. (a) Series of HAADF-STEM images after exposing the particle to the electron beam as a function of time. (b) STEM–EDX count rate maps of Cd, S, Si and the overlay of Cd and S of the obtained final shape after 280 s. All scale bars are 20 nm.

a behavior was seen for *in situ* heating experiments on gold and silver nanorods.[43] Despite the reduction of the electron beam exposure by parking the beam at the lower left corner or blanking it in between images, the influence of such a carbon shell cannot be neglected. Fig. 4b shows zoomed-in STEM images of the spot in (a). These images were taken subsequently after either changing the temperature or after an increased amount of time as indicated. Partial and complete evaporation of single NRs is highlighted by arrows. It can be observed that the NRs did not deform to spheroidal or spherical shapes prior to sublimation. The left over fragments kept their width after partial sublimation. It should be noted that some NRs exhibited small Cd segregated spots (one is marked by the white square) which is ascribed to the electron beam irradiation as they were not found for NRs that were heated without prior electron beam exposure (Fig. 4c).

In order to check the influence of the electron beam and circumvent the carbon shell creation, different windows on the heating chip were visited at 300 °C, 450 °C, 500 °C, 600 °C and 700 °C. These windows had not been exposed to the electron beam before. Examples of different heating windows at different heating times are shown in Fig. 4c. The sublimation also started around 450 °C but was more severe than observed in Fig. 4a. This indicates that indeed a carbon shell was protecting the particles in Fig. 4a. Interestingly, the NRs also broke into fragments as observed for fs-illumination. As mentioned in the main text, this is a result of the silica confinement as it was not observed for uncoated CdSe NRs.[30] Similarly to our work, these authors observed sublimation of CdSe NRs without deformation or chemical transformation of the NRs to spherical shapes. In agreement with that, work performed by Reichert *et al.* showed that CdSe and CdS NRs were compositionally stable up to 700 °C in an inert atmosphere.[44] Our findings and the observations of Hellebusch *et al.* and Reichert *et al.* strengthen our hypothesis that the deformation and chemical transformations upon laser irradiation are not a purely heat-induced effect. Heat was shown to speed up the radiation-induced effects though.[29]

A further proof that the observed transformations are radiation-induced is that the NRs transformed similarly under electron beam exposure. During the EDX and high-resolution STEM image acquisition we observed that part of the deformed fragments could also further deform under the electron beam. Furthermore, the segregated Cd sometimes appeared, grew or even dissolved again under the electron beam (Fig. S5†). A few about 1 nm or smaller Cd spots could also sometimes be observed at the surface of the undeformed NRs within the silica shell (Fig. S3†). This might stem from an excess of Cd-ions during the synthesis which were reduced by the electron beam and aggregated or alternatively from a slight evaporation of S or Se, but these dots are not enough to form the large bright Cd spots as observed after fs-illumination. Such a Cd segregation is energetically favoured over single Cd atoms and was also observed during *in situ* heating of CdSe/CdS octapods due to non-stoichiometric conditions.[45] A similar process is also known for Au on CdS NRs where isolated Au clusters were found to combine into one domain at the tip of the CdS NR upon heating.[37]

Due to the electron beam sensitivity of the nanorods we decided to follow the radiation-induced damaging and transformations of the CdSe/CdS NRs inside the silica shells *in situ* in the TEM under the impact of the electron beam (probe current of 506.4 μA). Fig. 5a shows a series of HAADF-STEM images as a function of e-beam irradiation time. First, the nanorod began to thin at one spot (35 s) where it then broke (70 s). Then, a second part thinned (70 s, 105 s) at which point the particle broke a second time (140 s, 175 s). The three fragments deformed further to a more spherical shape (210 s, 280 s). Additionally, a bright spot occurred after around 140 s at the highest fragment and grew further over time until it was bigger than the rest of the fragment (Fig. S6†). EDX measurements of the obtained fragments confirmed that the bright spot was Cd (Fig. 5b). Thus CdS must have decomposed as the CdS volume was decreasing whereas the Cd volume was increasing. As mentioned before, decomposition of CdS and agglomeration of Cd atoms as metallic Cd was observed earlier under the influence of an electron beam for Au-tipped CdS NRs.[29] EDX quantification of the elongated fragment at the bottom and the upper fragment with the segregated Cd revealed that while the elongated fragment had a Cd : S ratio of 53 : 47 (similar to undeformed NRs) the upper fragment showed a clear Cd excess with a Cd : S ratio of 74 : 26. This indicates that CdS was not only decomposing but that S must have sublimated or left the system otherwise.

By comparing the experiments under fs-laser and electron beam excitation it can be seen that the impact of both excitations is quite similar as the obtained shapes and resulting chemical compositions are alike. Since the particle in Fig. 5 first broke into rod-like fragments which afterwards deformed into more spherical shapes, we believe that the shape in the left image of Fig. 2b was formed at lower absorbed energies than the other two. The particles in the right column absorbed most energy from the laser fluence with respect to the other two and deformed further. Although the in-between shapes were observed for the same laser fluence it does not mean that all the particles absorbed exactly the same amount of energy. The fluences were calculated for the focal plane (see ESI†). Due to the high numerical aperture of the confocal setup, however, small inhomogeneities in height lead to differently absorbed energies, as described in more detail in ref. 25. Furthermore, the nanorods exhibit polarized absorption meaning that particles aligned with the laser polarization direction absorb more than the ones perpendicular to it.[46] For these reasons, particles lying in the illuminated area of about 12 μm × 12 μm experienced slightly different fluences leading to the different shapes.

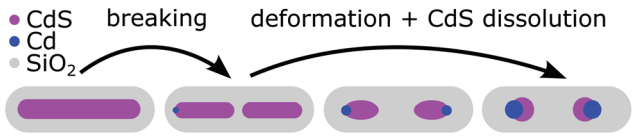

Fig. 6 Schematics of the observed deformation process.

The observed deformation mechanism is illustrated schematically in Fig. 6. The nanorods first break into two or more rod fragments. The individual fragments then deform *via* shorter rods to an eventually spherical shape. The fragments decrease in volume due to decomposition and sublimation of CdS. The left-over Cd atoms after CdS decomposition form metallic Cd which segregates at one end of the fragments. Left-over S most likely sublimated. However, it needs to be mentioned that not all fragments show metallic Cd spots. Finally, if more energy is absorbed, the NRs completely sublimate through the silica shell as seen the last column in Fig. 2a.

Conclusion

In conclusion, we studied the morphological and chemical transformations of silica-coated CdSe/CdS NRs. We found that the silica-coating enhanced the photostability under fs-pulses. Furthermore, the NRs transformed under the impact of fs-laser pulses or electron beam exposure by breaking into fragments which deformed to more spherical shapes. In the process, CdS partly decomposed which led to the segregation of metallic Cd. The resulting Cd and CdS crystals were found to have a well-defined orientation relationship and having an epitaxial interface between the crystals. The confinement by the silica shell played a critical role in this process as uncovered CdSe/CdS NRs were found to just sublimate without any transformations. Hence, there is still a lot to learn about the often out-of-equilibrium interaction of radiation and nanostructures. Novel nanostructures and epitaxial metal–semiconductor interfaces can be made by fs-laser excitation. These experiments show that fs-laser excitation opens a new way of nanoparticle tuning as it can transform the morphology and chemical composition in a controlled way in a small volume. They also raise questions, however, about the chemical and morphological stability when using these NRs in devices that are subject to application-related prolonged irradiation.

Author contributions

A. v. B. initiated and supervised the project. E. M. H. synthesized the particles under the supervision of D. V., W. A. performed the fs-laser experiments and TEM measurements on the same particles before and after excitation as well as the *in situ* heating experiments. B. G. performed the STEM and EDX measurements under the supervision of S. B., M. v. H. facilitated the *in situ* heating electron microscopy measurements and helped in explaining the experimental results. All authors discussed results and gave feedback on the written manuscript.

Acknowledgements

The authors acknowledge financial support from the European Research Council under the European Unions Seventh Framework Programme (FP-2007–2013)/ERC Advanced Grant Agreement 291667 HierarSACol. The authors furthermore acknowledge financial support from the European Research Council (ERC Starting Grant 335078-COLOURATOMS and ERC Consolidator Grant 683076 NANO-INSITU). The authors also appreciate financial support from the European Union under the Seventh Framework Program (Integrated Infrastructure Initiative No. 262348 European Soft Matter Infrastructure, ESMI). This work was supported by the Flemish Fund for Scientific Research (FWO Vlaanderen) through a postdoctoral research grant to B. G. The authors furthermore thank Dave J. van den Heuvel and Hans C. Gerritsen for use of the Thorlabs powermeter. We furthermore thank Ernest van der Wee for the simulation of the confocal point spread functions.

References

1 A. Sitt, F. Della Sala, G. Menagen and U. Banin, *Nano Lett.*, 2009, **9**, 3470–3476.
2 Y. Kelestemur, A. F. Cihan, B. Guzelturk and H. V. Demir, *Nanoscale*, 2014, **6**, 8509–8514.
3 Y. Yang, Y. Zheng, W. Cao, A. Titov, J. Hyvonen, J. R. Manders, J. Xue, P. H. Holloway and L. Qian, *Nat. Photonics*, 2015, **9**, 259–266.
4 C. Dang, J. Lee, C. Breen, J. S. Steckel, S. Coe-Sullivan and A. Nurmikko, *Nat. Nanotechnol.*, 2012, **7**, 335–339.
5 B. Guzelturk, Y. Kelestemur, K. Gungor, A. Yeltik, M. Z. Akgul, Y. Wang, R. Chen, C. Dang, H. Sun and H. V. Demir, *Adv. Mater.*, 2015, **27**, 2741–2746.
6 G. Xing, Y. Liao, X. Wu, S. Chakrabortty, X. Liu, E. K. L. Yeow, Y. Chan and T. C. Sum, *ACS Nano*, 2012, **6**, 10835–10844.
7 S. Halivni, A. Sitt, I. Hadar and U. Banin, *ACS Nano*, 2012, **6**, 2758–2765.
8 S. Deka, A. Quarta, M. G. Lupo, A. Falqui, S. Boninelli, C. Giannini, G. Morello, M. De Giorgi, G. Lanzani, C. Spinella, R. Cingolani, T. Pellegrino and L. Manna, *J. Am. Chem. Soc.*, 2009, **131**, 2948–2958.
9 L. Carbone, C. Nobile, M. De Giorgi, F. Della Sala, G. Morello, P. Pompa, M. Hytch, E. Snoeck, A. Fiore, I. R. Franchini, M. Nadasan, A. F. Silvestre, L. Chiodo, S. Kudera, R. Cingolani, R. Krahne and L. Manna, *Nano Lett.*, 2007, **7**, 2942–2950.
10 D. V. Talapin, R. Koeppe, S. Gotzinger, A. Kornowski, J. M. Lupton, A. L. Rogach, O. Benson, J. Feldmann and H. Weller, *Nano Lett.*, 2003, **3**, 1677–1681.
11 F. T. Rabouw, P. Lunnemann, R. J. A. van Dijk-Moes, M. Frimmer, F. Pietra, A. F. Koenderink and D. Vanmaekelbergh, *Nano Lett.*, 2013, **13**, 4884–4892.
12 A. Persano, M. De Giorgi, A. Fiore, R. Cingolani, L. Manna, A. Cola and R. Krahne, *ACS Nano*, 2010, **4**, 1646–1652.
13 K. Becker, J. M. Lupton, J. Müller, A. L. Rogach, D. V. Talapin, H. Weller and J. Feldmann, *Nat. Mater.*, 2006, **5**, 777–781.
14 A. E. Albers, E. M. Chan, P. M. McBride, C. M. Ajo-Franklin, B. E. Cohen and B. A. Helms, *J. Am. Chem. Soc.*, 2012, **134**, 9565–9568.
15 E. Khon, K. Lambright, R. S. Khnayzer, P. Moroz, D. Perera, E. Butaeva, S. Lambright, F. N. Castellano and M. Zamkov, *Nano Lett.*, 2013, **13**, 2016–2023.
16 T. O'Connor, M. S. Panov, A. Mereshchenko, A. N. Tarnovsky, R. Lorek, D. Perera, G. Diederich, S. Lambright, P. Moroz and M. Zamkov, *ACS Nano*, 2012, **6**, 8156–8165.
17 J. B. Rivest, S. L. Swisher, L.-K. Fong, H. Zheng and A. P. Alivisatos, *ACS Nano*, 2011, **5**, 3811–3816.
18 R. A. M. Hikmet, P. T. K. Chin, D. V. Talapin and H. Weller, *Adv. Mater.*, 2005, **17**, 1436–1439.
19 P. Zijlstra, J. W. M. Chon and M. Gu, *Nature*, 2009, **459**, 410–413.
20 G. Xing, S. Chakrabortty, K. L. Chou, N. Mishra, C. H. A. Huan, Y. Chan and T. C. Sum, *Appl. Phys. Lett.*, 2010, **97**, 061112.
21 G. Xing, S. Chakrabortty, S. W. Ngiam, Y. Chan and T. C. Sum, *J. Phys. Chem. C*, 2011, **115**, 17711–17716.
22 Y. Chen, J. Vela, H. Htoon, J. L. Casson, D. J. Werder, D. A. Bussian, V. I. Klimov and J. A. Hollingsworth, *J. Am. Chem. Soc.*, 2008, **130**, 5026–5027.
23 S. Jun and E. Jang, *Angew. Chem., Int. Ed.*, 2013, **52**, 679–682.
24 Y.-S. Chen, W. Frey, S. Kim, K. Homan, P. Kruizinga, K. Sokolov and S. Emelianov, *Opt. Express*, 2010, **18**, 8867–8878.
25 W. Albrecht, T.-S. Deng, B. Goris, M. A. van Huis, S. Bals and A. van Blaaderen, *Nano Lett.*, 2016, **16**, 1818–1825.
26 A. Imhof, M. Megens, J. J. Engelberts, D. T. N. de Lang, R. Sprik and W. L. Vos, *J. Phys. Chem. B*, 1999, **103**, 1408–1415.
27 A. van Blaaderen and A. Vrij, *Langmuir*, 1992, **8**, 2921–2931.
28 F. Pietra, R. J. A. van Dijk - Moes, X. Ke, S. Bals, G. Van Tendeloo, C. de Mello Donega and D. Vanmaekelbergh, *Chem. Mater.*, 2013, **25**, 3427–3434.

29 M. A. van Huis, A. Figuerola, C. Fang, A. Béché, H. W. Zandbergen and L. Manna, *Nano Lett.*, 2011, **11**, 4555–4561.
30 D. J. Hellebusch, K. Manthiram, B. J. Beberwyck and A. P. Alivisatos, *J. Phys. Chem. Lett.*, 2015, **6**, 605–611.
31 B. P. Khanal, A. Pandey, L. Li, Q. Lin, W. K. Bae, H. Luo, V. I. Klimov and J. M. Pietryga, *ACS Nano*, 2012, **6**, 3832–3840.
32 H. Petrova, J. Perez Juste, I. Pastoriza-Santos, G. V. Hartland, L. M. Liz-Marzán and P. Mulvaney, *Phys. Chem. Chem. Phys.*, 2006, **8**, 814–821.
33 E. M. Hutter, F. Pietra, R. J. A. Van Dijk - Moes, D. Mitoraj, J. D. Meeldijk, C. De Mello Donegá and D. Vanmaekelbergh, *Chem. Mater.*, 2014, **26**, 1905–1911.
34 A. Sitt, I. Hadar and U. Banin, *Nano Today*, 2013, **8**, 494–513.
35 W. Dallari, M. S. D'Abbusco, M. Zanella, S. Marras, L. Manna, A. Diaspro and M. Allione, *J. Phys. Chem. C*, 2012, **116**, 25576–25580.
36 G. Menagen, J. E. Macdonald, Y. Shemesh, I. Popov and U. Banin, *J. Am. Chem. Soc.*, 2009, **131**, 17406–17411.
37 A. Figuerola, M. A. van Huis, M. Zanella, A. Genovese, S. Marras, A. Falqui, H. W. Zandbergen, R. Cingolani and L. Manna, *Nano Lett.*, 2010, **10**, 3028–3036.
38 G. Bertoni, V. Grillo, R. Brescia, X. Ke, S. Bals, A. Catellani, H. Li and L. Manna, *ACS Nano*, 2012, **6**, 6453–6461.
39 W. G. J. H. M. van Sark, P. L. T. M. Frederix, A. A. Bol, H. C. Gerritsen and A. Meijerink, *ChemPhysChem*, 2002, **3**, 871–879.
40 X. Wen, A. Sitt, P. Yu, H.-c. Ko, Y.-R. Toh and J. Tang, *J. Nanopart. Res.*, 2012, **14**, 1278.
41 Y. Wu and P. Yang, *Adv. Mater.*, 2001, **13**, 520–523.
42 C. Burda, X. Chen, R. Narayanan and M. A. El-Sayed, *Chem. Rev.*, 2005, **105**, 1025–1102.
43 Y. Khalavka, C. Ohm, L. Sun, F. Banhart and C. Sönnichsen, *J. Phys. Chem. C*, 2007, **111**, 12886–12889.
44 M. D. Reichert, C.-C. Lin and J. Vela, *Chem. Mater.*, 2014, **26**, 3900–3908.
45 B. Goris, M. A. van Huis, S. Bals, H. W. Zandbergen, L. Manna and G. Van Tendeloo, *Small*, 2012, **8**, 937–942.
46 J. S. Kamal, R. Gomes, Z. Hens, M. Karvar, K. Neyts, S. Compernolle and F. Vanhaecke, *Phys. Rev. B: Condens. Matter*, 2012, **85**, 035126.